Front. Optoelectron. 2016, 9(3): 390–394
DOI 10.1007/s12200-016-0576-5

RESEARCH ARTICLE

Comparison of wavelength conversion efficiency between silicon waveguide and microring resonator

Meng XIONG (✉)[1], Yunhong DING[1], Haiyan OU[1], Christophe PEUCHERET[2], Xinliang ZHANG[3]

1 Department of Photonics Engineering, Technical University of Denmark, 2800 Kgs. Lyngby, Denmark
2 FOTON Laboratory, CNRS UMR 6082, ENSSAT, University of Rennes 1, F-22305 Lannion, France
3 Wuhan National Laboratory for Optoelectronics, Huazhong University of Science and Technology, Wuhan 430074, China

Abstract Wavelength conversion based on degenerate four-wave mixing (FWM) was demonstrated and compared between silicon nanowire and microring resonator (MRR). 15 dB enhancement of conversion efficiency (CE) with relatively low input pump power (5 mW) was achieved experimentally in an MRR. The impacts of bus waveguide length and propagation loss were theoretically analyzed under the effect of nonlinear loss.

Keywords wavelength conversion, four-wave mixing (FWM), silicon nanowaire, microring resonator (MRR)

1 Introduction

Silicon photonics has received increasing attention over the past decade for its inherent advantages, including ultra-compact size and compatibility with microelectronics fabrication processes [1,2]. Moreover, the high index contrast of silicon-on-insulator (SOI) makes it possible to confine the light tightly and therefore enhance nonlinearities, enabling to exploit silicon waveguides for all-optical signal processing applications, including parametric amplification, wavelength conversion, format conversion and optical switching [1,2]. In particular, wavelength conversion based on degenerate four-wave mixing (FWM) in waveguides (WGs) has been widely studied. Field enhancement in a resonant cavity, typically a microring resonator (MRR), can be applied to further increase the conversion efficiency (CE) or reduce the pump energy requirements through strengthening the nonlinear interaction between the optical waves [3,4].

However, nonlinear losses in silicon due to two-photon absorption (TPA) and TPA-induced free-carrier absorption (FCA) ultimately limit the wavelength CE in both WGs and MRRs. Furthermore, MRRs are typically accessed via bus waveguides in which the FWM process also takes place, making it difficult to assess the intrinsic benefit of the field enhancement in the MRR itself. High FWM CEs were achieved in MRRs with low input pump powers in Refs. [3,4]. However, a direct and quantitative comparison of CE in WGs and MRRs for a wide range of pump powers has, to the best of our knowledge, never been reported.

Recently, we have presented a theoretical comparison of FWM wavelength conversion in silicon WGs and MRRs [5], however, it was presented without any experimental result. In this paper, we first experimentally demonstrated enhanced CE in an MRR, and use the results to validate a numerical model. Based on the model, we quantified the relative CEs of silicon MRRs and WGs depending on the linear propagation losses.

2 Device fabrication

A 3.5 mm long WG and an MRR with the same bus length were fabricated on an SOI wafer with top silicon thickness of 250 nm and buried silica of 3 μm. The width and height for both straight and bend waveguides were 540 and 250 nm, respectively, which resulted in a dispersion value of -3 ps^2/m for the TE mode around 1550 nm. An MRR radius of 47 μm was chosen. MRRs with smaller radii have lower power requirements due to their smaller mode volumes, which also makes the free carriers build up faster and thus results in a lower CE [3]. High Q-factor MRRs enable the demonstration of FWM with ultra-low pump energies, but meanwhile suffer from narrow bandwidths, which limit the data rate at which optical signal processing is achievable [4]. To make the MRR applicable for signal processing at a bit rate of 10 Gb/s, a field coupling

Received December 25, 2015; accepted April 27, 2016

E-mail: xiongmeng2008@gmail.com

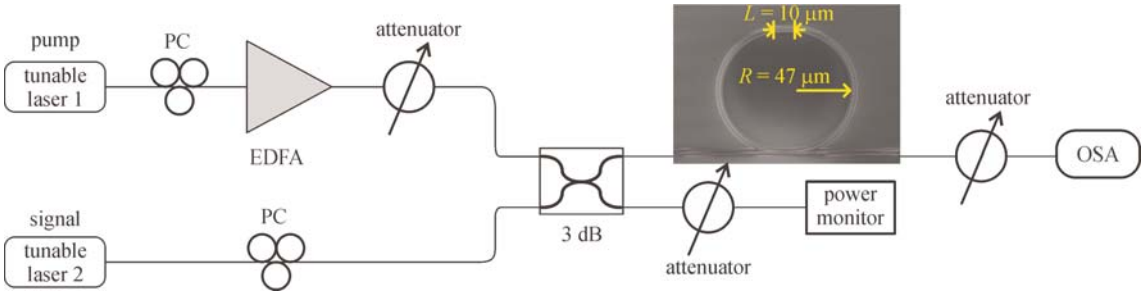

Fig. 1 Experimental setup for wavelength conversion

coefficient around 0.6 was preferred. Therefore the coupling length and gap between the ring and the bus waveguide were designed to be 10 μm and 90 nm, respectively.

The MRR and WG were fabricated using electron-beam lithography followed by inductively-coupled plasma reactive ion etching. The fabricated MRR structure was shown in Fig. 1. A silicon nano-taper was used to decrease the coupling loss between the device and tapered optical fibers. An insertion loss of 6 dB was achieved with a free space range (FSR) of 1.8 nm and an extinction ratio (ER) of 1.5 dB, corresponding to a field coupling coefficient of 0.54. The propagation loss of the WG was 2.6 dB/cm.

3 Experimental results

The experimental setup for wavelength conversion was shown in Fig. 1. Continuous wave (CW) light at 1548.19 nm was used as pump beam, while CW light at 1549.99 nm was used as the signal. Both the pump and signal lights were tuned to the resonances of the MRR and had their polarizations aligned to the TE mode of the waveguide thanks to polarization controllers (PCs). The pump light was amplified by an erbium-doped fiber amplifier (EDFA) followed by a tunable attenuator to control the pump power injected into the chip. The pump and signal lights were combined in a 3 dB coupler and launched into the MRR or WG.

Figure 2 shows the measured CE, which was defined as the ratio of the converted idler power at the device output to the signal power at its input (fixed at 0.1 mW), in both WG (triangle) and MRR (square), as a function of pump power. A CE as high as −30 dB can be achieved in the MRR with only 5 mW of pump power, which was 15 dB higher than that measured in the WG. However, the CE in the MRR quickly saturated with increasing pump power and the enhancement decreases to 5 dB when the pump power reached 50 mW.

4 Theoretical model

To simulate the FWM process in WGs and MRRs, a theoretical model solving a system of three coupled differential equations for the complex envelopes of the pump, signal and idler, and taking TPA and FCA into account, was used [6]. This model is valid as long as higher-order idlers are negligible, which is typically the case in silicon waveguides at the power levels considered in this study. The nonlinear index, TPA coefficient and effective mode area were taken equal to 6×10^{-18} m^2/W, 5×10^{-12} m/W and 0.1 μm^2, respectively. Due to the small wavelength separation between the interacting waves, the effect of dispersion above second order was neglected. The MRR was modeled according to Ref. [7]. Free carrier lifetimes of 4 ns for the MRR and 3 ns for the WG were adopted here for the devices used in the experiment. The simulated results in Fig. 2 show good agreement with the experimental characterizations.

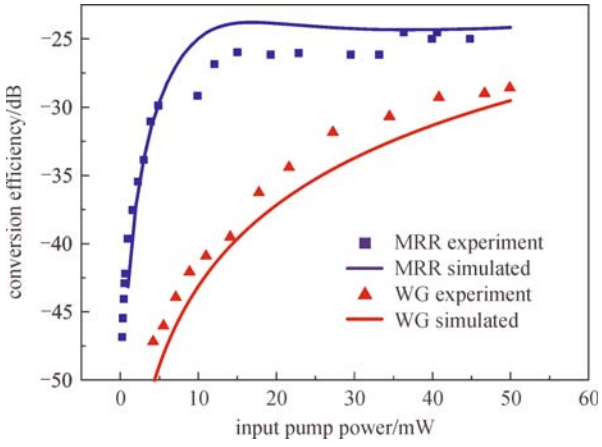

Fig. 2 Measured (square symbols for MRR and triangles for WG) and simulated (blue curve for MRR and red curve for WG) CE as a function of input pump power

5 Discussion

The CEs in WGs strongly depend on their lengths and linear losses. By optimizing the geometry of the WG, dispersion close to zero and shorter carrier lifetime can be achieved for both MRRs and WGs. The CEs of WGs were calculated as a function of pump power for different linear

loss values with -0.3 ps^2/m dispersion and 1 ns carrier lifetime. For each linear loss value, an optimum waveguide length that further depends on the pump power (via nonlinear absorption mechanisms) can be found, as shown in Fig. 3. The maximum CE decreases with increasing linear loss. In addition, the optimum length is reduced with increasing pump power due to TPA and FCA. In the following, three different optimum waveguide lengths are considered for the bus, depending on the linear loss (33 mm for 1 dB/cm, 11 mm for 3 dB/cm and 6 mm for 5 dB/cm), corresponding to maximized CEs.

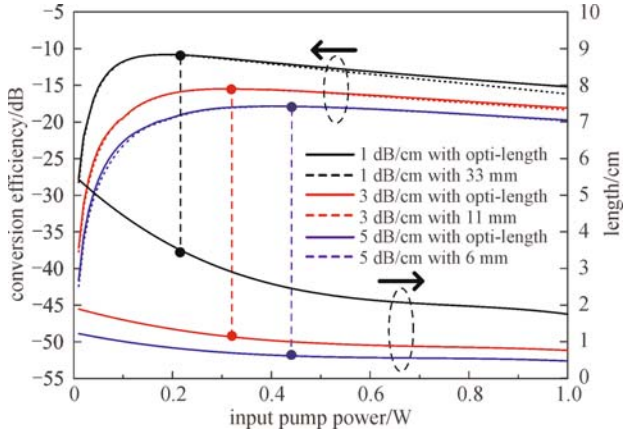

Fig. 3 Left axis: CE as a function of pump power for WGs with optimal (solid lines) and fixed (dashed line) lengths and different linear losses. Right axis: optimal WG length as a function of pump power

Figure 4 shows the calculated CE of an MRR with the same radius and coupling coefficient as in the experiments. The results were also compared with those of a straight WG of same length as the bus. To evaluate the performances of the MRR and WG at higher pump powers, a maximum power of 0.3 W was used in the simulation, which was much higher than that in the experiment. At high input pump powers, the CEs of the WG and MRR were almost the same regardless of the linear loss. This is because the pump field enhancement of the MRR gives rise to higher TPA and FCA losses in the ring. However, at low pump powers, the CE of the MRR was obviously larger than that of the WG. The pump power resulting in a given CE was smaller in the MRR than in a WG of same length as the bus, and the improvement was more significant for larger loss. This is due to the fact that the enhancement of the pump power in the MRR is not high enough to induce obvious nonlinear loss.

To assess the intrinsic benefit of the field enhancement in the MRR itself, the CE of a MRR without the bus was calculated and compared with that of a straight WG of the same length as the circumference of the MRR, i.e., 0.3 mm. A maximum CE improvement of around 33–34 dB can be achieved depending on the linear losses, as shown in Fig. 5. However, the CE of the MRR begins to decrease after the pump power was over 50 mW. As a matter of fact, with the increasing of the input pump power, the CE of both MRR and WG will saturate and even drop if the TPA

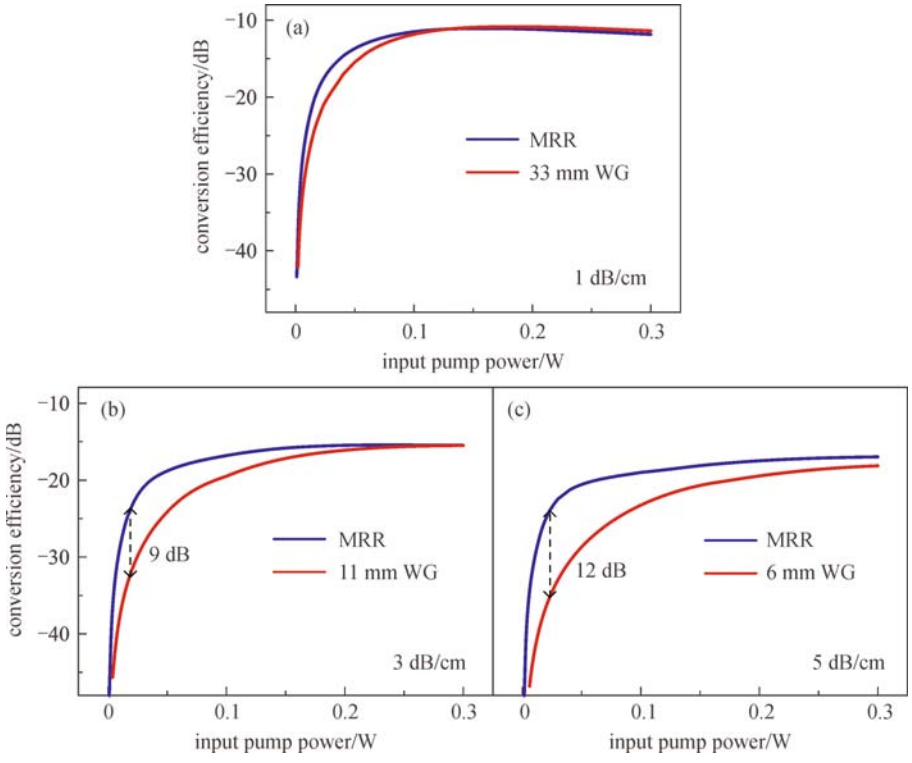

Fig. 4 CEs of WGs of different lengths with and without MRR for different linear loss values, (a) 1 dB/cm; (b) 3 dB/cm; (c) 5 dB/cm

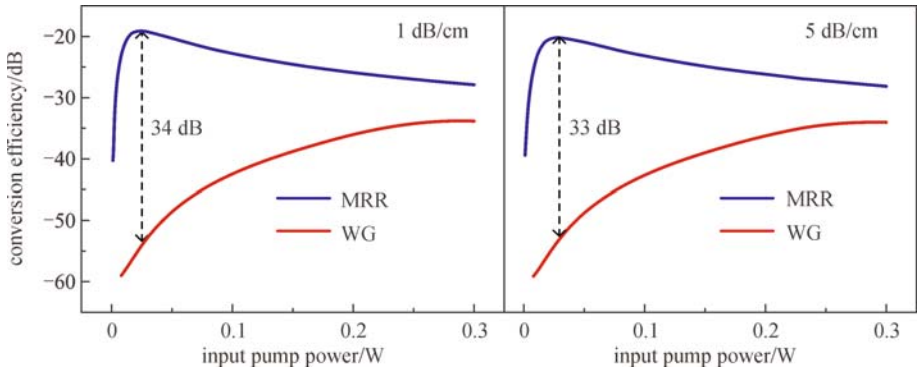

Fig. 5 CEs of MRRs (without bus waveguide) and WGs of the same length as the circumference of the MRRs for two different linear losses of 1 and 5 dB/cm

and FCA become dominate effects in the waveguides. Since it is more obvious for MRR due to its high Q value, the maximum CE of WG will be higher than that of MRR with a certain propagation loss and waveguide length under strong input power. And besides, the enhancement of CE for MRR with a low Q value will become non-obvious when it is compared to WG.

6 Conclusion

Wavelength conversion based on degenerate FWM in silicon WGs and MRRs has been experimentally and theoretically analyzed. Compared to a WG having the same length as that of the bus of the MRR, the CE in the MRR can be improved as much as 15 dB at low pump powers.

References

1. Foster M A, Turner A C, Sharping J E, Schmidt B S, Lipson M, Gaeta A L. Broad-band optical parametric gain on a silicon photonic chip. Nature, 2006, 441(7096): 960–963
2. Oxenløwe L K, Ji H, Galili M, Pu M, Hu H, Mulvad H C H, Yvind K, Hvam J M, Clausen A T, Jeppesen P. Silicon photonics for signal processing of Tbit/s serial data signals. IEEE Journal of Selected Topics in Quantum Electronics, 2012, 18(2): 996–1005
3. Turner A C, Foster M A, Gaeta A L, Lipson M. Ultra-low power parametric frequency conversion in a silicon microring resonator. Optics Express, 2008, 16(7): 4881–4887
4. Li F, Pelusi M, Xu D X, Ma R, Janz S, Eggleton B J, Moss D J. All-optical wavelength conversion for 10 Gb/s DPSK signals in a silicon ring resonator. Optics Express, 2011, 19(23): 22410–22416
5. Xiong M, Ding Y, Ou H, Peucheret C, Zhang X. Systematic comparison of FWM conversion efficiency in silicon waveguides and MRRs. In: Proceedings of OptoElectronics and Communications Conference, 2013, TuPM-7
6. Lin Q, Painter O J, Agrawal G P. Nonlinear optical phenomena in silicon waveguides: modeling and applications. Optics Express, 2007, 15(25): 16604–16644
7. Li Z, Gao S, Liu Q, He S. Modified model for four-wave mixing-based wavelength conversion in silicon micro-ring resonators. Optics Communications, 2011, 284(8): 2215–2221

Meng Xiong received the B.Sc. and Ph.D. degrees from College of Optoelectronic Science and Engineering, Huazhong University of Science and Technology (HUST), China, in 2008 and 2013, respectively. Her Ph.D. project is design, fabrication of microring resonators and their applications in all-optical signal processing. She was working as a postdoc in DTU Fotonik in 2015. She is currently a R&D engineer in Light Extraction Aps. in Denmark, working on the surface patterning of more efficient LED.

Yunhong Ding received the B.Sc. degree from College of Optoelectronic Science and Engineering, Huazhong University of Science and Technology (HUST), China, in 2006, as well as the Ph.D. degree from this same university in 2011. His Ph.D. project dealt with micro-ring resonators for lossless all optical buffers. He was a guest Ph.D. student at the Technical University of Denmark between 2009 and 2011, where he was involved in the fabrication, characterisation and system tests of silicon microring resonators. He was working as a postdoc in DTU Fotonik since 2011. He is involved in the EU SEQUOIA project (ref. no. FP7-619626, 2013 – 2016), and he is the grant holder of national DFF Sapere Aude project (ref. no. DFF–1335-00771, 2013 – 2016) and FTP-project SimcROADM (ref. no. DFF–1337-00152, 2013 – 2016). His broad expertise ranges from components design and fabrication to high-speed system demonstrations using those devices. He is currently a researcher fellow at the Technical University of Denmark, working on silicon integrated devices for space division multiplexing and quantum information processing.

Haiyan Ou received the Ph.D. degree in semiconductor devices and microelectronics from the Institute of Semiconductors, Chinese Academy of Sciences (CAS) in 2000. From 2000, she joined Technical University of Denmark, where she was promoted as associate professor in 2005. She has been a JSPS (Japanese Society for Promotion of Science) fellow at Meijo University (Japan), and a visiting professor at the Institute of Semiconductors, CAS (China). Her scientific background is in the areas of materials and devices for optical communication, photovoltaics, and light emitting. She has published more than 160 journal and conference papers, and is the founder of Light Extraction ApS.

Christophe Peucheret received the graduate engineering degree from Telecom Bretagne, Brest, France, the M.Sc. degree in microwaves and optoelectronics from University College London, London, UK, and the Ph.D. degree from the Technical University of Denmark (DTU), Copenhagen, Denmark. He has been with the Department of Photonics Engineering at the Technical University of Denmark between 1997 and 2013. Since September 2013 he is with the FOTON Laboratory (CNRS UMR 6082), ENSSAT, University of Rennes 1, Lannion, France. His research interests are in the area of all-optical signal processing for optical communication and interconnect applications, in particular utilizing parametric processes in nonlinear fibres and waveguides, silicon photonic devices, and the applications of micro-resonators and nanophotonic components.

Xinliang Zhang received the Ph.D. degree in physical electronics from Huazhong University of Science and Technology (HUST), Wuhan, China, in 2001. He is currently with the Wuhan National Laboratory for Optoelectronics and the School of Optical and Electronic Information, HUST, as a Professor. He is the author or coauthor of more than 400 journal and conference papers. His current research interests include all-optical signal processing and related components.